Journal of Applied Science and Engineering Methodologies
Volume.2, No.3, (2016): Page.311-316
www.scientistlink.com/jasem

Characterization of polycrystalline p-type transparent conducting $CuFeO_2$ thin films prepared by chemical spray pyrolysis technique

E. Ashlyn Kirupa[a,*], A. Moses Ezhil Raj[b]

[a]Department of Physics & Research Centre, Nesamony Memorial Christian College, Marthandam - 629 165, India
[b]Department of Physics & Research Centre, Scott Christian College (Autonomous), Nagercoil - 629 003, India

Abstract

Transparent mixed oxide transparent conducting thin films ($CuFeO_2$) have been successfully deposited on glass substrates at 300 ^oC by spray pyrolysis deposition without any post-deposition annealing. Thickness of the films was varied by changing the proportion of cation's molar concentrations viz. 0.1:0.1, 0.15:0.15, 0.2:0.2 M. The XRD peak positions of the films confirmed the hexagonal (rhombohedral) $CuFeO_2$ single and polycrystalline phase structure. The surface morphology of $CuFeO_2$ thin film seems relatively smooth and crack free; the EDX spectra confirmed the stoichiometry of the prepared films. The oxidation state of the cations Cu, Fe and the anion O; and their chemical environment were analyzed in an X-ray photoelectron spectrometer. The binding energies of Cu-2p doublet positioned at 932.7 eV and 952.6 eV, along with its satellites represented the existence of Cu^{2+} in the films. Additional peaks located at binding energies 709.3 and 723.4 eV corresponds to the Fe-2p of the film that dictated the presence of Fe^{2+} in the compound. The direct band gap of the film infers the presence of an intermediate band in between the band edges due to Fe 3d states. The p-type conductivity and conductivity variations with temperature confirmed the semiconducting nature of the films. The activation energy decreases from 0.483 to 0.438 eV as the thickness of the film increases.

Keywords: P-type semiconductor- XRD – XPS – Optical – Electrical

*Corresponding Author: E. Ashlyn Kirupa | e-mail: jenkiru1@yahoo.co.in | Mobile: 9865210715

1. Introduction

Delafossites are ternary oxides with the basic formula ABO_2, where A represents monovalent cations such as Cu or Ag, and B represents trivalent metals ranging from Al to La [1, 2]. Delafossite compounds have engrossed much interest due to their unusual magnetic and conducting properties for many years [3–5]. The cuprous delafossite ternary oxides ($CuBO_2$) exhibit semiconducting properties and the copper valencies either in Cu^I or Cu^{II} govern transport properties in delafossite compounds [6, 7]. $CuFeO_2$ is a p-type TCO that has relatively higher electrical conductivity compared with most of the delafossites and have been extensively studied due to their promising applications in transparent diodes and solar cells [8]. Few researchers have attempted to prepare $CuFeO_2$ thin films by using techniques such as pulsed laser deposition [9], radio-frequency (RF) sputtering [10,11] and sol-gel [12]. For the first time, present study reports the deposition and characterization of p-type $CuFeO_2$ thin films on glass substrates by using spray pyrolysis processing.

2. Experimental Details

Copper Iron oxide nanostructures were spray pyrolytically synthesized on well cleaned glass substrates using copper chloride [$CuCl_2$] (M.W.=170.48) and Ferric chloride [$FeCl_3$] (M.W.=162.21) dissolved in 50% ethanol (C_2H_5OH) and de-ionized water for various Cu:Fe concentrations, 0.1:0.1, 0.15:0.15 and 0.2:0.2 M at the constant substrate temperatures of 300 ^oC. The solution was then sprayed on the glass substrates at the solution flow rate of 0.5 ml/sec using a carrier gas flow of 0.3 kg/cm^2. The thickness of the films was measured using Stylus profiler. The X-ray diffraction patterns of $CuFeO_2$ films were obtained with an X-ray diffractometer (XPERT-PRO) using CuKα (30mA, 40kV, λ=1.54060) at a continuous scan type with step size 0.0330 (^{0}2Th). The surface properties of all films were investigated using JEOL Model JSM-6390LV Scanning electron microscope. The chemical environment of the $CuFeO_2$ films was investigated using VG Microtech Multilab ESCA 3000 spectrometer with a non-monochromatized M_g K_α X-ray source at the vacuum level of 10^{-10} Torr. The optical properties were measured with UV-NIR Spectrometer (Varian make model Cary5000) in the wavelength range 250 –1050 nm. The two probe technique was used for measuring electrical resistivity of $CuFeO_2$ films.

3. **Results and Discussion**

Fig. 1 shows the XRD pattern of $CuFeO_2$ thin films deposited using precursors of various concentrations. The diffraction peaks located at $2\theta=33.5^o$ and $2\theta=38.6^o$ corresponds to (1 0 1) and (1 0 4) reflection of $CuFeO_2$ phase in the rhombohedral R-3m (N-166) space group using the hexagonal axes. The peak positions were matched with the standard rhombohedral phase which was similar to those reported by Adel et al [13]. Calculated lattice parameters, unit cell volume and density are in good agreement with the JCPDS standards (No: 75-2146). Other related structural parameters such as crystallite size, microstrain and dislocation density of the films are listed in Table 1.

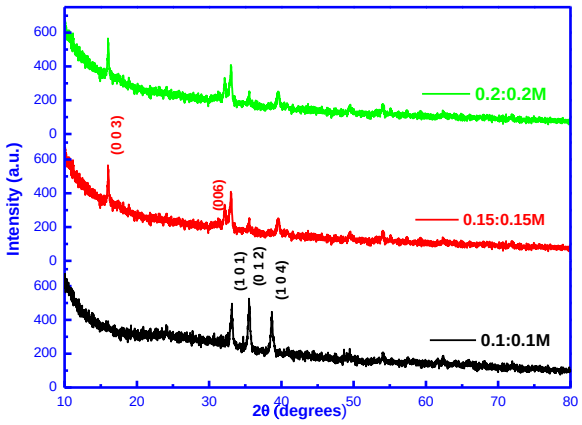

Fig. 1 XRD pattern of $CuFeO_2$ thin films deposited using precursors of various concentrations

Table 1 Calculated structural parameters of $CuFeO_2$ thin films

Cu:Fe concentrations (M)	Lattice parameters (Å)	Volume ($Å^3$)	Density (g/cm^3)	Crystallite size (nm)	Microstrain ($*10^{-3}$)	Dislocation density ($*10^{14}$ lines/m)
0.1:0.1	a=3.0395 c=17.776	142.22	5.3010	51.8	0.628	3.73
0.15:0.15	a=3.1734 c=16.287	142.00	5.3091	43.4	0.697	5.30
0.2:0.2	a=3.1603 c=16.432	142.09	5.3057	28.7	1.158	12.10

With increasing film thickness, usually the grain size increases that lead to introduce fewer defects in the crystal lattice. However in the present study, grain size decreases with increase in film thickness, which may be due to the realignment of crystal basis especially in the (003) and (006) planes. Initiated growth in those planes diminishes the XRD intensity of the prominent planes (012) and (104). This embarked variation not only increases the defects parameters but also changes the surface morphology of the grains as evidenced form the SEM micrographs.

Fig. 2 shows the SEM micrograph of $CuFeO_2$ films prepared using precursors of various concentrations. The films deposited using solution concentration 0.1:0.1 M are composed of compact crystallites with irregular facades and the close connection of the grains without any voids provide continuous pathways that ease propagation of the charge carriers. The films deposited at the concentration of 0.15:0.15 M appear to be porous due to the connection between grains is loose. The nano crystallites of higher concentration are not highly homogeneous in shape and size, since the crystallites coalesce together to form grains with larger size.

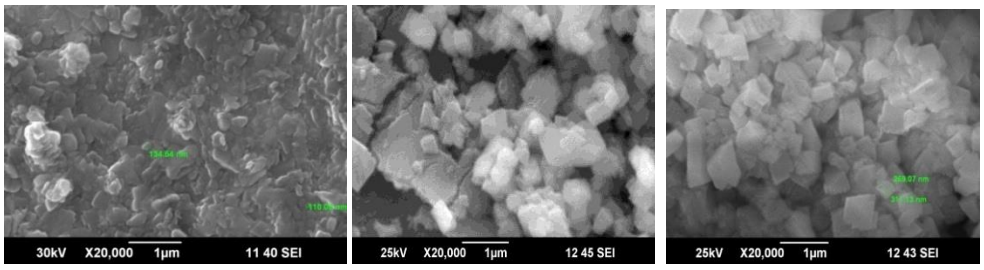

(a) (b) (c)

Fig. 2 SEM micrograph of $CuFeO_2$ films deposited using precursors of different concentrations (a) 0.1:0.1 M (b) 0.15:0.15 M (c) 0.2:0.2 M

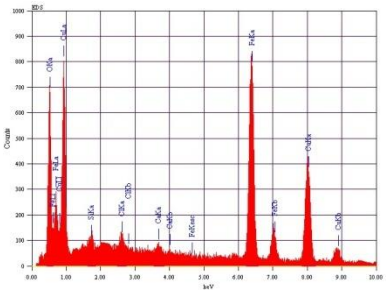

Fig. 3 shows the EDAX spectrum of the optimised film. It clearly confirms the purity of the prepared film by revealing major peaks corresponding to Cu, Fe and O. The incorporation of other elements Ca (0.72%), Cl (1.29%) and Si (0.7%) in feeble amount is unavoidable as the film substrate is glass.

Fig. 3 EDAX Spectrum of $CuFeO_2$ thin films

The XPS core level spectrum of Cu 2p is displayed in Fig. 4, which includes four peaks at 932.7, 940.5, 952.6, and 961.4 eV. The peak at 932.7 eV corresponds to Cu $2p_{3/2}$ and the one at 952.6 corresponds to Cu $2p_{1/2}$. The two other peaks on the higher binding energy side of both $Cu2p_{3/2}$ and $Cu2p_{1/2}$ are satellite structures. These satellites can be attributed to shakeup transitions by ligand-to-metal 3d charge transfer. This charge transfer can occur for copper if it present in Cu^{2+} form ($3d^9$ configurations). Further it reveals the nonexistence of copper in but cannot metallic or in Cu^{+} state ($3d^{10}$ configurations), because of their completely filled 3d shells [14–16].

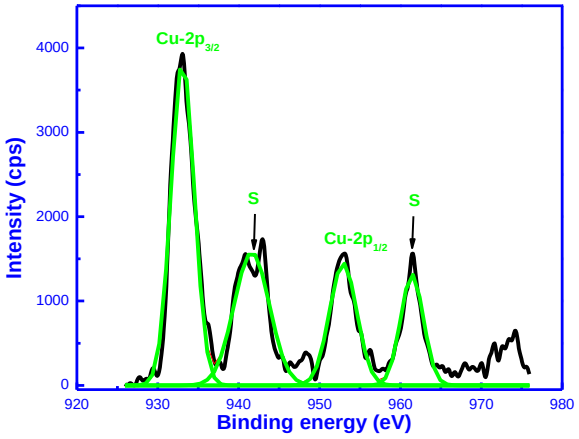

Fig. 4 Core level spectrum of Cu-2p

From the XPS scan of Fe 2p shown in Fig. 5, the position of Fe $2p_{3/2}$ and Fe $2p_{1/2}$ peaks are located at 709.3 and 723.4 eV respectively. The satellite peak for Fe $2p_{3/2}$ was observed at 715.6. The binding energy difference between the Fe $2p_{3/2}$ peak and the satellite peak is 6.3 eV. It was evident that a satellite occurring at approximately 6.0 eV above the Fe $2p_{3/2}$ peak is the characteristic of the presence of Fe^{2+} species. The presence of this satellite peak and the binding energy difference clearly proves the existence of Fe^{2+}. Obtained results are reliable with those obtained by other researchers [17-21], lending good support to confirm the formation of $CuFeO_2$ with cations Cu

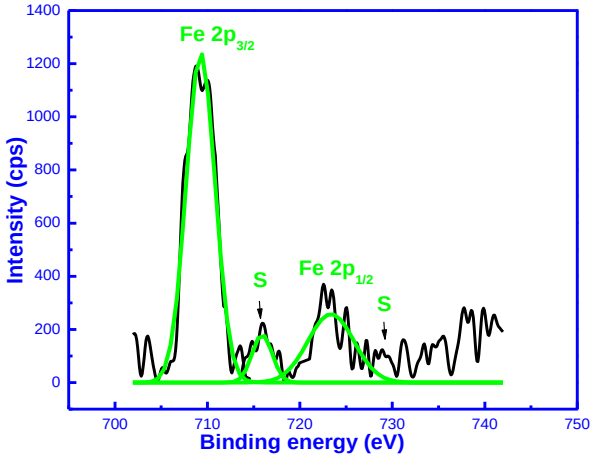

Fig. 5 High resolution XPS scan of Fe-2p

and Fe, both are in the +2 ionized state.

After curve deconvolution, the O 1s spectrum shown in Fig. 6 reveals two components corresponding to various chemical states of oxygen [22]. The main peak located at 528.9 eV corresponds to the lattice oxygen [23] and other nearby peak in the high energy side at 530.2 eV corresponds to the adsorbed hydroxyl groups (M–OH). The study clearly indicates the formation of $CuFeO_2$ with cations in the ionized state of +2 and surface is sensitive to

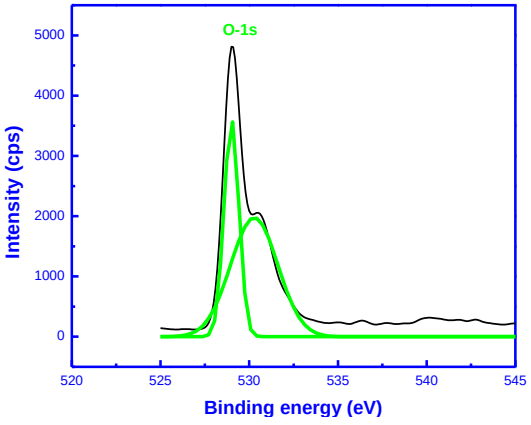

Fig. 6 High resolution XPS scan of O -1s

atmospheric moisture that are adsorbed to the material.

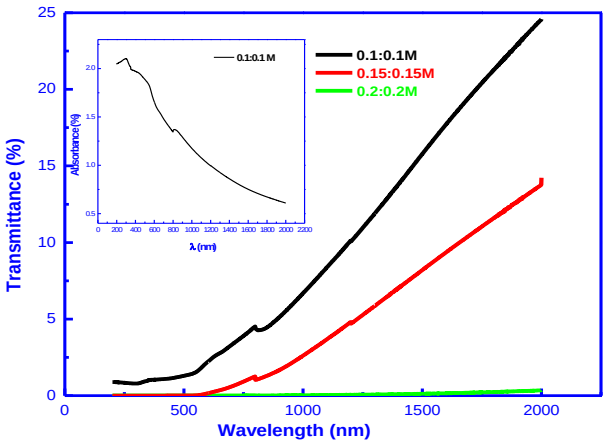

Fig. 7 Optical transmittance of $CuFeO_2$ films deposited using precursors of different

The optical transmittance curve of $CuFeO_2$ films deposited using precursors of different concentrations are shown in Fig. 7. The transmittance decreases with increasing solution concentration due to the increase in thickness of the films. As the material content increases, covalent bonds between Cu, Fe and oxygen also increases which in turn decreases the transmittance of the incident light especially at the shortest wavelengths. The electrons in the outer orbits have transferred to the higher energy levels and occupied vacant positions of energy bands. Thus, a part of incident light does not penetrate through it [24]. Also at higher concentration, the grain density is large and hence grain boundary scattering is large which in turn results poor transmittance.

The inlet of Fig. 7 shows the optical absorption spectrum of optimized $CuFeO_2$ film. As observed, absorption bands are visible at 282, 338, 478 and 818 nm that corresponds to the various charge-transfer (CT) excitations to the TM 3*d* orbitals. Presence of many absorption edges commonly reported in $CuFeO_2$, may be due to the appearance of an intermediate band due to Fe 3d states in the wide band gap usually present between the flat valence band originated in Cu 3d states and corresponding high energy conduction band of typical delafossite oxides [25- 27]. These absorptions bands are assigned to the transitions Cu 3d → Cu $3d_z^2$ + 4s, Cu 3d → Fe e_g , Cu 3d →Fe t_{2g} and Cu 3d →Fe t_{2g} respectively [28- 30]. Charge transfer interactions are again confirmed through the determination of the optical band gap 'Eg' by constructing a plot between $(\alpha h\nu)^2$ against hν (Fig. 8). A linear relationship between $(\alpha h\nu)^2$ and hν indicates that $CuFeO_2$ has direct energy band gap. Similar to absorption edges, there appear four optical bands respectively at 4.39, 3.67, 2.59, 1.52 eV.The optical direct band gap for the films deposited using precursor concentration 0.1:0.1 M shows the band gap values of 1.44, 2.06, 3.12 eV , which are increases to 1.91, 2.60 eV and 2.99 eV for the films deposited using solution concentration 0.15:0.15 M. Obtained values are comparable to the previously reported results values [31- 37]. The increase in energy band gap for the higher concentrations can be attributed to the decreasing of the crystallite size and the deterioration of the crystallinity of the films as evidenced from the XRD pattern.

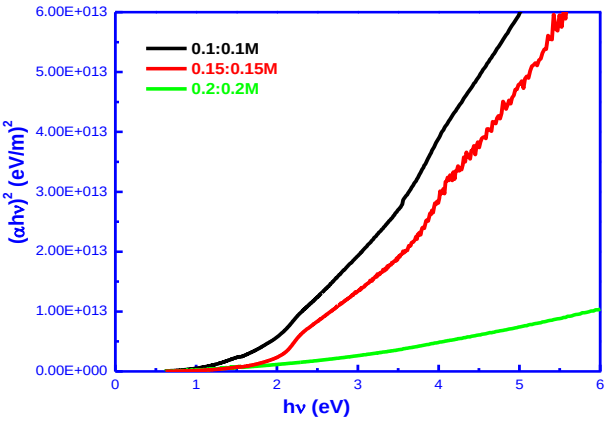

Fig. 8 Tauc plot of $CuFeO_2$ films deposited using precursors of different concentrations

The electrical conductivity of the films was recorded using the two probe technique. The conductivity of films is moderate and increases with temperature. The increase in conductivity is linked with a hopping mechanism which is favoured with the oxygen intercalation in the Cu^{2+} layers of the delafossite ($CuBO_2$). For smaller B cation like Fe, oxygen intercalation is forcible and generates structural shear and defects [38]. Above a critical oxidation degree, the delafossite structure cannot accept any more oxygen anions. The electrical conductivities of prepared films are still low compared to bulk reference. This is due to the defect structure generated by the forced oxygen intercalation and by the thin film microstructure [39]. The activation energy E_a was determined from the slope of the Arrhenius plot given in Fig. 9. The activation energy decreases from 0.483 eV, 0.440 eV, and 0.438 eV for the films 0.1:0.1 M, 0.15:0.15 M, and 0.2:0.2 M respectively with the increase in the film thickness.

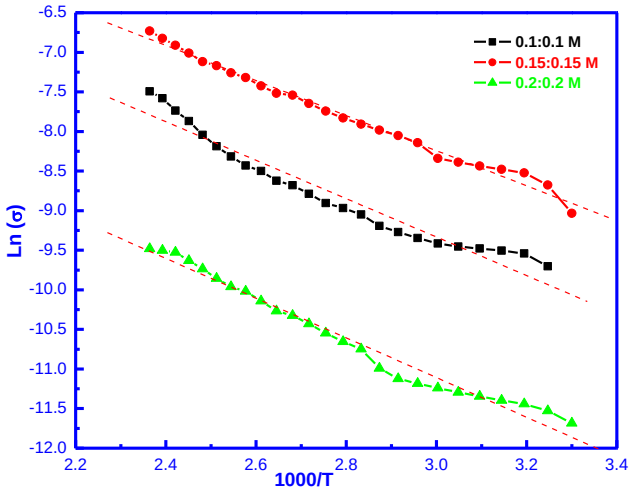

Fig. 8 Arrhenius plot of $CuFeO_2$ films deposited using precursors of different concentrations

Conclusions

Copper Iron oxide thin films have been prepared using the chemical spray pyrolysis technique on glass substrates. Films deposited at the optimized Cu:Fe concentration ratio (0.1:0.1M) and at the substrate temperature (300 ^oC) revealed well crystalline nature indexed for the rhombohedral phase. The diffraction peaks located at $2\theta=33.5^o$ and $2\theta=38.6^o$ corresponds to (1 0 1) and (1 0 4) reflection of $CuFeO_2$ phase. As the concentration ratio increases with the film thickness the crystallinity of the film decreases due to covalent bonding and hence the defect parameters dominate. Surface examination by SEM revealed the formation of particles which uniformly covered the entire glass substrate. XPS spectra confirmed that the observed Cu 2p, Fe 2p and the O1s peaks correspond to the $CuFeO_2$ nanostructures. Optical absorption studies showed the presence of direct band transitions in $CuFeO_2$ thin films which confirmed the charge transfer interactions for the optimised thin film. The conductivity variations confirmed the semiconducting nature of the films.

References

[1] H.Y. Chen, J.H. Wu, Appl. Surf. Sci. 258 (2012) 4844.
[2] H.F. Jiang, C.Y. Gui, Y.Y. Zhu, D.J. Wu, S.P. Sun, C. Xiong, X.B. Zhu, J. Alloys Compd. 582 (2014) 64.
[3] D.B. Rogers, R.D. Shannon, C.T. Prewitt, J.L. Gillson, Inorg. Chem. 10 (1971) 723.
[4] F.A. Benko, F.P. Koffyberg, J. Phys. Chem. Solids 45 (1984) 57.
[5] J.P. Doumerc, A. Wichainchai, A. Ammar, M. Pouchard, P. Hagenmuller, Mater. Res. Bull. 21 (1986) 745.
[6] B.J. Ingram, T.O. Mason, R. Asahi, K.T. Park, A.J. Freeman, Phys. Rev., B 64 (2001) 155114-1.
[7] G. Thomas, Nature 389 (1997) 907.
[8] M. M. Moharam, M. M. Rashad, E. M. Elsayed, R. M. Abou Shahba , Journal of Materials Science: Materials in Electronics 25 (2014) 1798.

[9] D.H. Choi, S.J. Moon, J.S. Hong, S.Y. An, I.-B. Shim, C.S. Kim, Thin Solid Films 517 (2009) 3987.
[10] A. Barnabé, E. Mugnier, L. Presmanes, P. Tailhades, Mater. Lett. 60 (2006) 3468.
[11] E. Mugnier, A. Barnabé, L. Presmanes, P. Tailhades, Thin Solid Films 516 (2008) 1453.
[12] Hong-Ying Chen, Jia-Hao Wu Thin Solid Films 520 (2012) 5029.
[13] Adel H.Omran Alkhayatt , S. M.Thahab , Inass Abdulah Zgair Applied Numerical Mathematics and Scientific Computation Nov (2014) 165.
[14] B. Wallbank, I.G. Main, C.E. Johnson, J. Electron Spectrosc. 5 (1) (1974) 259.
[15] K.S. Kim, J. Electron Spectrosc. 3 (3) (1974) 217.
[16] J.F. Watts, J. Wolstenholme, An Introduction to surface analysis by XPS and AES, Wiley, 2003 (Chapter 3.2.5).
[17] Toru Yamashita, Peter Hayes Applied Surface Science 254 (2008) 2441.
[18] S.J. Roosendaal, B. van Asselen, J.W. Elsenaar, A.M. Vredenberg, F.H.P.M. Habraken, Surf. Sci. 442 (1999) 329.
[19] P.C.J. Graat, M.A.J. Somers, Appl. Surf. Sci. 100 (1996) 36.
[20] P. Mills, J.L. Sullivan, J. Phys. D: Appl. Phys. 16 (1983) 723.
[21] M. Muhler, R. Schlo¨gl, G. Ertl, J. Catal. 138 (1992) 413.
[22] F. Parmigiani, P.S. Bagus, G. Pacchioni,Cluster Models for Surface and bulk phenomena, Plenum, New York, 1992, pp. 475.
[23] H.Y. Chen, D.J. Hsu, J. Alloys Compd. 598 (2014) 23.
[24] R. Suresh, V. Ponnuswamy, and R. Mariappan Int. J. Thin Fil. Sci. Tec. 4, No. 1, (2015) 35.
[25] G. Riveros, C. Garín, D. Ramírez, E.A. Dalchiele, R.E. Marotti, C.J. Pereyra, E. Spera, H. Gómez, P. Grez, F. Martín, J.R. Ramos-Barrado Electrochimica Acta 164 (2015) 297.
[26] K.P. Ong, K. Bai, P. Blaha, P. Wu, Chem. Mater. 19 (2007) 634.
[27] X.L. Nie, S.H. Wei, S.B. Zhang, Phys. Rev. Lett. 88 (2002) 066405.
[28] F. A. Benko and F. P. Koffyberg, Mater. Res. Bull. 21 (1986) 753.
[29] K. P. Ong, K. Bai, P. Blaha, and P. Wu, Chem. Mater. 19 (2007) 634.
[30] Hiroki Hiraga, Takayuki Makino, Tomoteru Fukumura, Hongming Weng, and Masashi Kawasaki Physical Review B 84 (2011) 041411
[31] C.G. Read, Y. Park, K.S. Choi, J. Phys. Chem. Lett. 3 (2012) 1872.
[32] A. Derbal, S. Omeiri, A. Bouguelia, M. Trari, Int. J. Hydrogen Energy 33 (2008) 4274
[33] Z.H. Deng, X.D. Fang, S.Z. Wu, W.W. Dong, J.Z. Shao, S.M. Wang, M. Lei, J. Sol–Gel Sci. Technol. 71 (2014) 297.
[34] A. Barnabe, E. Mugnier, L. Presmanes, P. Tailhades, Mater. Lett. 60 (2006) 3468.
[35] F.A. Benko, F.P. Koffyberg, J. Phys. Chem. Solids 48 (1987) 431.
[36] H.Y. Chen, J.H. Wu, Appl. Surf. Sci. 258 (2012) 4844
[37] R.K. Gupta, M. Cavas, A.A. Al-Ghamdi, Z.H. Gafer, F. El-Tantawy, F. Yakuphanoglu, Sol. Energy 92 (2013) 1.
[38] E. Mugnier, A. Barnabé and Ph. Tailhades, Solid State Ionics 177 (2006) 607.
[39] S. Capdeville, P. Alphonse, C. Bonningue, L. Presmanes and P. Tailhades, J. Appl. Phys. 96 (2004) 6142.